Organometallics **1993,** *12,* 76–80

π-Acidity of Thioethers and Selenoethers: Truth or Fiction? A Comparative Density Functional Study

Heinz-Bernhard Kraatz, Heiko Jacobsen, Tom Ziegler,* and P. Michael Boorman

*Department of Chemistry, University of Calgary, 2500 University Drive, NW,
Calgary, Alberta, Canada T2N 1N4*

Received May 14, 1992

Using density functional theory (DFT) within the local density approximation (LDA), the electronic and geometrical structure of octahedral $(OC)_5Cr{-}L$ with L = CO, NR_3, PR_3, AsR_3, SR_2, SeR_2 (N, P, As, R = F, H; S, Se, R = F, H, Me), and OR_2 (R = H, Me) were studied. All structures have been optimized in C_s symmetry. The resulting geometries are rationalized in terms of orbital interactions. The metal–ligand bond energy has been determined for all systems in calculations where nonlocal corrections were added to the LDA energy expression. It was possible to break down the total metal–ligand bond energy into contributions stemming from σ-donation and π-back-bonding; hence, it is possible to rank thioethers and selenoethers in terms of σ-donor and π-acceptor ability. In general, thio- and selenoethers are rather poor π-acceptors and weak σ-donors. The methyl-substituted chalcogenoethers are better σ-donors than the chalcogenhydrides. It is found that the fluoro-substituted chalcogen systems exhibit good π-acceptor abilities, comparable to those found for PF_3. Surprisingly, the fluorine substitution does not significantly decrease the σ-donor ability. The Cr–E bond energies increase in the order $Cr{-}EH_2 < Cr{-}EMe_2 < Cr{-}EF_2$ (E = O, S, Se).

Introduction

The relevance of thioether–transition metal complexes as possible intermediates in the hydrodesulfurization of fossil fuels[1] has prompted numerous investigations into the structure and reactivity of transition metal–thioether complexes, as well as its heavier congener selenoether.[2] Many of them provide evidence suggesting that thioethers have some π-acceptor ability.[2c–f] Although the bonding of other ligands, like phosphines, to metal centers has received considerable theoretical attention,[3] the bonding between thio- and selenoethers and transition metals has been neglected until recently[4] in *quantitative* theoretical studies. We reported that thioethers in the bridging position of d^3–d^3 bioctahedral complexes use their σ^*-orbitals to accept electron density from the metal center.[4] Previous attempts to quantify σ-donor and π-acceptor behavior using vibrational spectroscopy have been a matter of some contention,[5] due to the difficulty of separating σ-, π-, and synergic effects. However, it has been of some merit for a comparative overall (σ–π) bonding evaluation for a variety of ligands.[6] The prime focus of our investigation is the characterization of the electronic properties of thio- and selenoether ligands in terms of σ-donating and π-accepting abilities and the *quantitative* comparison of our findings to the bonding characteristics of widely used ligands, such as carbon monoxide, phosphines, arsines, and ethers. The metal system of choice is $(OC)_5Cr$, since it has received wide attention from theoreticians and experimentalists alike. We have excluded OF_2 from our discussion, since our calculations suggest that it does not show simple coordination chemistry.[7]

Density functional theory (DFT) within the local density approximation (LDA)[8b] has been proven to accurately predict geometrical structures and to give reliable estimates of the ligand bond dissociation energies in transition metal complexes[8a,b] after the addition of nonlocal corrections. Applying the generalized transition state method[9] allows a detailed analysis of the calculated bonding energies and a breakdown into steric and electronic contributions. The electronic contributions can be broken down further (vide infra), and this allows us to describe π- and σ-contributions to the bonding separately.

Computational Details

All calculations were based on approximate density functional theory within the local density approximation,[10] LDA, in the parametrization by Vosko et al.[11] In addition, we used Becke's[12] nonlocal exchange correction as well as inhomogenous gradient corrections for correlation due to Perdew.[13] The reported

---

(1) Lesch, D. A.; Richardson, J. W.; Jacobson, R. W.; Angelici, R. J. *J. Am. Chem. Soc.* **1984,** *106,* 2901.

(2) (a) Murray, S. G.; Hartley, F. R. *Chem. Rev.* **1981,** *81,* 365 and references therein. (b) Boorman, P. M.; Gao, X.; Fait, J. F.; Parvez, M. *Inorg. Chem.* **1991,** *30,* 3886. (c) Baker, E. N.; Larsen, N. G. *J. Chem. Soc., Dalton Trans.* **1976,** 1769. (d) Sellman, D.; Lechner, P.; Knoch, F.; Moll, M. *J. Am. Chem. Soc.* **1992,** *114,* 922. (e) Cotton, F. A.; Zingales, F. *Inorg. Chem.* **1962,** *1,* 145. (f) Weiner, M. A.; Lattman, M. *Inorg. Chem.* **1984,** *17,* 1084.

(3) (a) Xiao, S.-X.; Trogler, W. C.; Ellis, D. E.; Berkovich-Yellin, Z. B. *J. Am. Chem. Soc.* **1983,** *105,* 7033. (b) Marynick, D. S. *J. Am. Chem. Soc.* **1984,** *106,* 4064. (c) Lichtenberger, D. L.; Jatcko, M. E. *Inorg. Chem.* **1992,** *31,* 451.

(4) Jacobsen, H.; Kraatz, H.-B.; Ziegler, T.; Boorman, P. M. *J. Am. Chem. Soc.* **1992,** *114,* 7851.

(5) (a) Haines, L. M.; Stiddard, M. H. B. *Adv. Inorg. Chem. Radiochem.* **1969,** *12,* 53. (b) Boorman, P. M.; Clow, S. A.; Poots, D.; Wieser, H. *Inorg. Nucl. Chem. Lett.* **1973,** *9,* 941.

(6) (a) Cotton, F. A. *Inorg. Chem.* **1964,** *3,* 702. (d) Graham, W. A. G. *Inorg. Chem.* **1968,** *7,* 315.

(7) Kraatz, H.-B.; Jacobsen, H.; Ziegler, T.; Boorman, P. M. To be published.

(8) (a) Ziegler, T.; Tschinke, V.; Ursenbach, C. *J. Am. Chem. Soc.* **1987,** *109,* 4825. (b) Ziegler, T. *Chem. Rev.* **1991,** *91,* 651 and references quoted therein.

(9) (a) Ziegler, T.; Rauk, A. *Theor. Chim. Acta* **1977,** *46,* 1. (b) Baerends, E. J.; Rozendaal, A. *NATO ASI* **1986,** *C176,* 159.

(10) (a) Gunnarsson, O.; Lundquist, I. *Phys. Rev.* **1974,** *B10,* 1319. (b) Gunnarsson, O.; Lundquist, I. *Phys. Rev.* **1976,** *B13,* 4274. (c) Gunnarsson, O.; Johnson, M.; Lundquist, I. *Phys. Rev.* **1979,** *B20,* 3136.

(11) Vosko, S. J.; Wilk, M.; Nusair, M. *Can. J. Phys.* **1980,** *58,* 1200.

(12) (a) Becke, A. *J. Chem. Phys.* **1986,** *84,* 4524. (b) Becke, A. *J. Chem. Phys.* **1988,** *88,* 1053.

(13) (a) Perdew, J. P. *Phys. Rev.* **1986,** *B33,* 8822. (b) Perdew, J. P. *Phys. Rev.* **1986,** *B34,* 7406 (erratum).

0276-7333/93/2312-0076$04.00/0

Table I. Structural Parameters (deg, pm) of Optimized Structures of the Formula $(OC)_5CrER_3$ (E = N, P, As; R = H, F) and $(OC)_5CrER_2$ (E = S, Se, R = H, F, Me; E = O, R = H, Me)

ligand	no.	α	β	γ	d(Cr–E)	d(Cr–C$_t$)	d(C$_t$–O$_t$)	d(E–R)
$(OC)_5CrCO$	I	180.0	90.0		196.2	196.2	114.7	
$(OC)_5CrNH_3$	II	179.8	89.9	106.3	210.3	192.6	115.0	103.3
$(OC)_5CrPH_3$	III	175.0	87.5	97.6	225.4	194.4	114.6	142.4
$(OC)_5CrAsH_3$	IV	174.7	87.3	96.7	242.8	193.3	114.9	153.1
$(OC)_5CrOH_2$	V	175.52	92.2	103.2	218.0	191.6	115.2	98.6
$(OC)_5CrSH_2$	VI	178.2	90.9	89.7	234.0	193.8	115.0	136.7
$(OC)_5CrSeH_2$	VII	177.6	90.3	87.7	245.3	192.7	114.9	149.3
$(OC)_5CrNF_3$	VIII	176.5	91.7	99.3	192.9	194.3	114.3	139.4
$(OC)_5CrPF_3$	IX	174.7	92.6	97.4	215.3	196.1	114.3	156.1
$(OC)_5CrAsF_3$	X	170.8	94.6	95.4	232.9	194.4	114.5	174.8
$(OC)_5CrSF_2$	XI	179.1	90.5	92.0	212.4	196.2	114.1	165.2
$(OC)_5CrSeF_2$	XII	178.3	90.9	91.2	223.6	196.9	114.1	180.2
$(OC)_5CrOMe_2$	XIII	180.0	90.0	116.0	221.5	191.2	115.3	143.8
$(OC)_5CrSMe_2$	XIV	170.3	94.8	96.2	234.9	193.1	114.9	184.4
$(OC)_5CrSeMe_2$	XV	171.0	94.5	91.8	242.5	192.1	115.0	198.3

calculations were performed utilizing the vectorized version of the AMOL program system developed by Baerends et al.[14] and vectorized by Ravenek.[15] The numerical integration procedure applied for the calculations was developed by Boerrigter and te Velde.[16] All molecular structures were optimized within the C_s symmetry group. The geometry optimization procedure was based on the method developed by Versluis and Ziegler.[17] A double-ζ-STO basis set[18] was employed for the ns and np shells of the main group elements. The basis was augmented by a single 3d STO function except for hydrogen, where we used a 2p STO as polarization. The ns, np, nd, $(n+1)$s, and $(n+1)$p shells of chromium were presented by a triple-ζ-STO basis. Electrons in lower shells were considered as core and treated according to the procedure due to Baerends et al.[14] An auxiliary[19] set of s, p, d, f, and g STO functions, centered on all nuclei, was used in order to fit the molecular density and present Coulomb and exchange potentials accurately in each SCF cycle. All calculations were spin restricted. All structures were optimized at the LDA level of theory. The calculated bond energies include nonlocal corrections evaluated from LDA densities.[8]

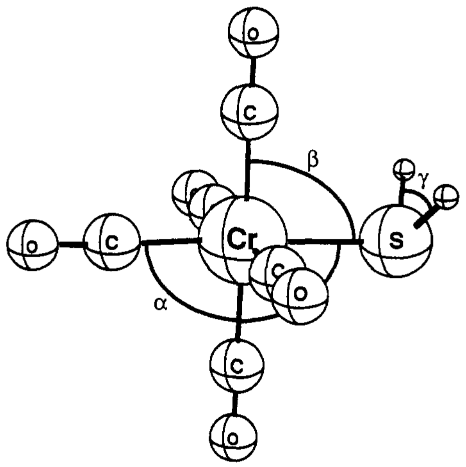

Figure 1. Optimization parameters for the $(OC)_5Cr–SH_2$ complex.

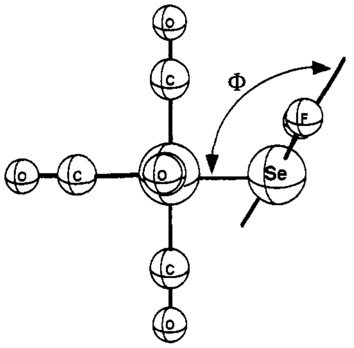

Complex	Φ (in °)
$(OC)_5CrOH_2$	108.1
$(OC)_5CrSH_2$	112.9
$(OC)_5CrSeH_2$	113.0
$(OC)_5CrSF_2$	117.5
$(OC)_5CrSeF_2$	113.4
$(OC)_5CrOMe_2$	170.5
$(OC)_5CrSMe_2$	120.0
$(OC)_5CrSeMe_2$	116.9

Figure 2. Tilt-angle Φ of the chalcogenoether complexes.

Results and Discussion

Description of the Geometrical Structures. The $(OC)_5Cr–L$ systems with L = CO, NR_3, PR_3, AsR_3, SR_2, SeR_2 (for N, P, As, R = F, H; for S, Se, R = F, H, Me), and OR_2 (R = H, Me) have been structurally optimized in C_s symmetry (see Figure 1). Table I shows some structural parameters of the optimized complexes. As expected, the chromium–ligand distance is influenced by the substituent on the ligand L. Complexes of fluorinated ligands have a much shorter Cr–E distance, compared to complexes with methyl or hydrogen substituents. The chalcogenide ligands are bonded to the chromium center with a tilt away from the plane defined by the axial carbonyl ligands (Figure 2). This tilt-angle Φ is the largest for XIII.

The angle α, which is the angle between the trans-carbonyl group and the chalcogenide or pnictogenide ligand, becomes more acute as the steric demand of the substituent on the ligand increases. In the case of the methyl-substituted chalcogenide ligands, the trans carbonyl and the substituents adopt an anti conformation. The variation in the angle between the axial carbonyls and the ligand is less drastic but still influenced by the steric demand of the substituent.

Upon coordination, the chalcogenide and pnictogenide ligands undergo distortions as illustrated in Figure 2. We shall deal with the electronic factors responsible for the deformations later and simply specify the geometrical changes in the present section. A lengthening of the E–R bond compared to that of the free ligand (see Table II) is observed for most of the ligands. This lengthening is less significant for R = H and Me but of sizeable magnitude for R = F. For ER_2 systems (E = O, S, Se; R = H, F), the R–E–R angle gets more acute, which is in accordance with the observed behavior.[20]

The structure of the $Cr(CO)_5$ fragment is also influenced by the coordination of an additional ligand L. In particular,

---

(14) Baerends, E. J.; Ellis, D. E.; Ros, P. *Chem. Phys.* **1973**, *2*, 41.

(15) (a) Baerends, E. J. Ph.D. Thesis, Vrije Universitet, Amsterdam, 1975. (b) Ravenek, W. In *Algorithms and Applications on Vector and Parallel Computers*; Riele, H. J. J., Dekker, Th. J., van de Vorst, H. A., Eds.; Elsevier: Amsterdam, 1987.

(16) Boerrigter, P. M.; te Velde, G.; Baerends, E. J. *Int. J. Quantum Chem.* **1988**, *33*, 87.

(17) Versluis, L.; Ziegler, T. *J. Chem. Phys.* **1988**, *88*, 322.

(18) (a) Snijders, G. J.; Baerends, E. J.; Vernooijs, P. *At. Nucl. Data Tabl.* **1982**, *26*, 483. (b) Vernooijs, P.; Snijders, G. J.; Baerends, E. J. Slater Type Basis Functions for the whole Periodic System. Internal report, Free University of Amsterdam, Netherlands, 1981.

(19) Krijn, J.; Baerends, E. J. Fit functions in the HFS-method. Internal report, Free University of Amsterdam, Netherlands, 1984.

Table II. Comparison between the Bond Lengths (in pm) and Angles (in deg) of Free and Complexed Optimized Ligands

	complexed ligand		free ligand (calc)		free ligand (expt)[a]	
ligand	*d*(E–R)	R–E–R	*d*(E–R)	R–E–R	*d*(E–R)	R–E–R
CO	114.8		113.1			
NH_3	115.0	105.7	101.7	107.8	101.2	106.7
PH_3	142.3	96.9	142.0	93.9	142.00	93.345
AsH_3	153.0	95.2	151.9	91.8	151.1	92.1
OH_2	98.6	103.2	98.7	103.8	95.75	104.51
SH_2	136.7	89.7	135.6	91.6	133.56	92.12
SeH_2	149.3	87.7	146.6	90.4	146	91
NF_3	139.4	99.3	137.4	101.6	137	102.5
PF_3	156.1	97.4	157.7	97.7	157.0	97.8
AsF_3	174.8	95.4	175.6	95.4	171.0	95.9
SF_2	165.2	92.0	162.0	99.9	159.21	98.20
SeF_2	180.2	91.2	175.7	96.0		
OMe_2	143.8	116.0	143.4	115.7	141.6	112
SMe_2	184.4	96.2	183.7	96.6	180.7	99.05
$SeMe_2$	198.3	91.8	199.0	91.6	194.3	96.2

[a] All experimental values except those for SeH_2 and NF_3 were taken from: *CRC Handbook of Chemistry and Physics*, 72nd ed.; Lide, D. R., Ed.; CRC Press: Boca Raton, FL, 1992. Values for SeH_2 and NF_3: Greenwood, N. N.; Earnshaw, A. *Chemistry of the Elements*; Pergamon Press: Oxford, U.K., 1984.

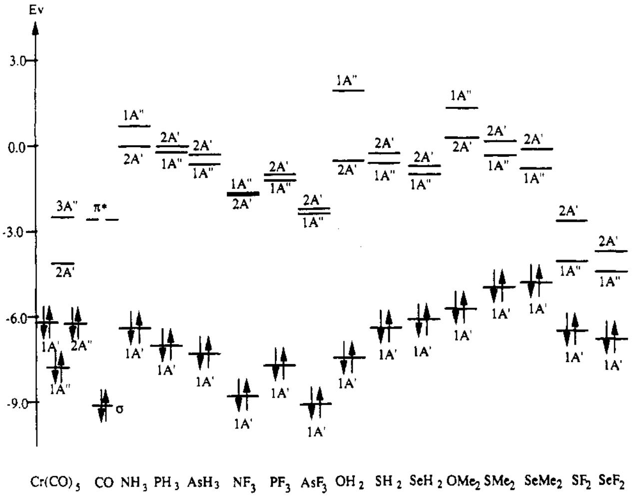

Figure 3. Frontier orbital levels of the metal and the ligand fragments.

the length of the bond between the metal atom and the trans carbonyl carbon is sensitive to the incoming ligand (Table I). For most of the ligands, except SF_2 and SeF_2, a shortening of the $Cr–C_t$ bond length is observed. Changes in the trans carbonyl C–O distance are minor (±0.6 pm) but significant. We shall shortly relate changes in the $Cr–C_t$ and $C_t–O_t$ distances to the π-acceptor strength of the chalcogenide and pnictogenide ligands.

Electronic Structures. The bonding involved can be conveniently analyzed by looking at the interaction between the two fragments $Cr(CO)_5$ and L. The frontier orbitals on the square pyramidal d^6-metal fragment consist of three fully occupied nonbonding orbitals 1A″ (d_{xy}) (**1a**), 2A″ (d_{xz}) (**1b**), and 1A′ (d_{yz}) (**2**) as well as the two empty orbitals 2A′ (d_{z^2}) (**3**) and 3A′ ($d_{x^2-y^2}$) at higher energies (see Figure 3).

The ligands have an occupied p-type donor orbital of 1A′ symmetry (**4a,b**) and two unoccupied σ^*-orbitals 2A′ (**5a,b**) and 1A″ (**6a,b**). Here the ER_3 acceptor orbital **6a** is one component of a degenerate set of acceptor orbitals with e-symmetry.

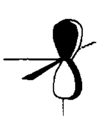

1a

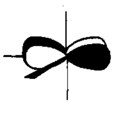

1b

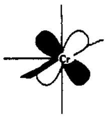

2

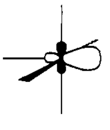

3

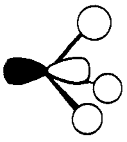

4a

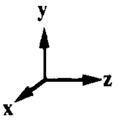

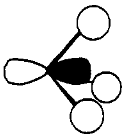

5a

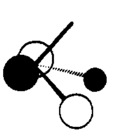

6a

4b

4c

5b

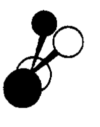

6b

The occupied ligand orbitals **4a,b** are donating electron density into the empty 2A′ orbital (**3**) on the metal fragment which is mainly made up of Cr d_{z^2} with some contribution from Cr p_z in order to maximize the interaction with the incoming ligand orbital, as shown in **7a** for L = ER_2. The chalcogen ligand orbital responsible for the donation in **7a** is mainly a chalcogen p-hybrid lone pair orbital, with some contributions from the substituent in the case of R = F and CH_3. The interaction in **7a** is at its maximum for a tilt-angle Φ of 90°. However, the ER_2 ligands coordinate in most cases to the metal fragment with tilt angles somewhat larger (Figure 2). The increase in Φ from 90° reduces the interaction in **7a** but allows at the same time for an interaction between the the 2A′ acceptor orbital (**3**) on the metal and the E–R σ-bonding orbital (**4c**) on the ligand, as shown in **7b**. The E–R σ-bonding orbital **4c** is of lower energy than the 1A′ (**4b**) lone pair orbital and thus less readily available for donation. Simple trigonometric considerations[21] indicate that the combined bonding overlaps are enhanced by a partial increase in Φ from 90°. The fact that Φ is larger for R = F and CH_3 than for R = H is attributed to steric factors. We note in particular an abnormal increase of Φ to 170° in the case of L = $O(CH_3)_2$.

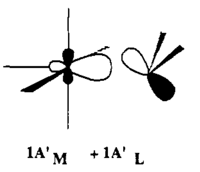

7a

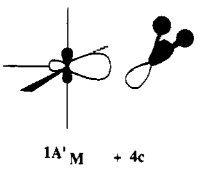

7b

There are two major metal–ligand interactions, which can be described as π-back-bonding to the ligand. The first of these interactions is shown in **8** for L = ER_2. It can be described as back-bonding from the metal d_{yz}-orbital, **2**, to a σ^*-orbital, **5b**, of the ligand. The second back-bonding interaction between the metal's d_{xy}-orbital, **1b**, and the second σ^*-orbital, **6b**, is shown in **9**, again for L = ER_2. The corresponding interactions with L = ER_3 would involve **5a** and **6a**, respectively.

The makeup of these σ^*-orbitals is strongly substituent dependent with an understandably large polarization

---

(20) (a) Moynihan, K. J.; Gao, X.; Boorman, P. M.; Fait, J. F.; Freeman, G. K. W.; Thornton, P.; Ironmonger, D. J. *Inorg. Chem.* **1990**, *29*, 1648. (b) Boorman, P. M.; Gao, X.; Freeman, G. K. W.; Fait, J. F. *J. Chem. Soc., Dalton Trans.* **1991**, *30*, 3886.

(21) Gimarc, B. M. In *Molecular Structure and Bonding*; Academic Press: New York, 1979.

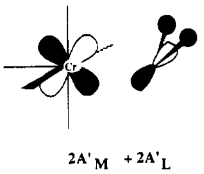

8

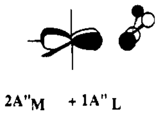

9

toward the chalcogen in the fluoro systems; see Table III. The σ*-orbital **6b** has in general a larger contribution on the chalcogen than **5b**, and it is thus not surprising that the acceptor strength of the σ*-orbital **6b**, according to a Mulliken population analysis, is higher (by an average factor of 2) than the more substituent-based σ*-orbital **5b**.

As mentioned above, coordination of the chalcogen ethers to the metal fragment leads to geometric changes of the ligand. Back-bonding in the case of sulfur- and selenium-based ligands will populate the σ*-orbital **6b**. In order to minimize the antibonding interaction between the orbitals of the substituent and the d-polarized p-orbital of the chalcogen, the R–E–R angle (E = S, Se) will have to decrease. A donation into both σ*-orbitals results in addition in a lengthening of the E–R bond. The calculated geometries of complexed and free ligands are compared in Table II. The calculated decrease in the R–E–R angle and lengthening of the E–R bond for all sulfur- and selenium-based ligands is in accordance with experiment.[2,20] For phosphorus- and arsenic-based ligands, complexation leads primarely to an increase in the R–E bond distance as the **5a** and **6a** σ*-orbitals are occupied (Table II).

Bond Analysis and Energy Decomposition. Using the generalized transition-state method,[9] we are able to separate steric and electronic contributions to the metal–ligand bond energy according to

$$\Delta H_{\mathrm{LA}} = -[\Delta E_{\mathrm{prep}} + \Delta E^{\circ} + \Delta E_{\mathrm{el}}] \qquad (1)$$

Here ΔH_{LA} represents the ligand association energy, with ΔE_{prep} being the energy required to deform the fragments from their equilibrium energy to the conformation in the complex. ΔE° is the steric interaction energy, which has a purely electrostatic component and an exchange repulsion term taking into account the destabilizing two-orbital four-electron interactions between occupied orbitals on both fragments. ΔE_{el} represents the stabilizing electronic contributions due to orbital interactions between an empty orbital on one fragment and an occupied orbital on the other fragment.

To obtain a detailed picture of the donation and back-bonding portions of the fragment interactions and to separate them from synergic effects, we chose to carry out calculations using molecular orbitals (MO's) constructed not as linear combinations of atomic orbitals but rather as linear combinations of fragment orbitals. This allows us to decompose the electronic contribution to the bond energy, ΔE_{el}, into contributions from σ-donation, ΔE_{σ}, π-back-bonding, ΔE_{π}, synergic contributions, ΔE_{syn}, and residual contributions, ΔE_{res}, according to

$$\Delta E_{\mathrm{el}} = \Delta E_{\sigma} + \Delta E_{\pi} + \Delta E_{\mathrm{syn}} + \Delta E_{\mathrm{res}} \qquad (2)$$

By allowing only one bonding type at a time, that is π-back-bonding to the ligand or σ-donation to the metal fragment, we can specifically address donor and acceptor qualities of each ligand. Removal of all unoccupied fragment orbitals from the metal fragment, but including only the two unoccupied acceptor orbitals of the ligand (**5a,b** (2A′) and **6a,b** (1A″)) allows us to extract the π-component, ΔE_{π}. On the other hand, the σ-component, ΔE_{σ}, representing the donor strength of the ligand is obtained by removing all unoccupied fragment orbitals from the ligand and leaving the one σ-acceptor orbital (**3** (2A′)) on the metal fragment. The donor and acceptor strengths of the ligand so obtained do not take into account the synergic nature of the interaction. A measure of the synergic effect, ΔE_{syn}, can be obtained from the extra stabilization gained by allowing for the three interactions **7–9** to take place at the same time. Finally, allowing all virtual orbitals, that is all the remaining unoccupied fragment orbitals on the ligand and the metal fragment, to participate affords the additional term ΔE_{res}.

The preparation energies are small, as is expected for simple coordination complexes. Due to the somewhat larger geometric changes of fluorine-substituted chalcogenoether systems, ΔE_{prep} is larger compared to the methyl- and hydrogen-substituted systems.

Table IV summarizes the results of our analysis. As expected, the donor strength of the chalcogenoether increases going down the group. It is worth pointing out that there is a significant increase on going from oxygen-based ligands to sulfur- or selenium-based ligands. Methyl-substituted chalcogenoethers are clearly better σ-donors than are the hydrogen-substituted ligands. Surprisingly, the donor strength of the fluorine-substituted chalcogenoethers is not reduced. In fact, they appear to have the same donor strength as the methyl derivatives.

The Mulliken population analysis for the nonsynergetic cases shows that acceptance of electron density into the σ*-orbitals of sulfur- and selenium-based ligands contributes a sizable amount to the overall orbital interaction. The ability to act as a π-acceptor is about the same for methyl- and hydrogen-substituted chalcogenoethers. For the fluorine-systems, the π-back-bonding ability experiences a 3-fold increase, compared to the methyl and hydrogen systems. This can be rationalized by looking at the acceptor orbitals on these two ligands. In both cases, **5b** and **6b** are largely chalcogen-based and this allows for a maximum overlap between **1** and **6b** and **2** and **5b**. The back-bonding ability of SF_2 and SeF_2 under nonsynergetic conditions even exceeds that of CO! For the pnictogenides, the effect of fluorine substitution is also evident but less pronounced. PF_3 is clearly a stronger π-acceptor than PMe_3 and PH_3, but the donor ability is slightly reduced. The oxygen-based ligands do not show any π-acceptor

Table III. Makeup of Chalcogen Ligand Donor and Acceptor Orbitals 5b and 6b

orbital	OH_2	SH_2	SeH_2	SF_2	SeF_2	OMe_2	SMe_2	$SeMe_2$
5b	1% O_s 6% O_p 93% subst	5% S_s 18% S_p 77% subst	4% Se_s 24% Se_{p_y} 72% subst	65% S_p 5% S_d 30% subst	5% Se_s 66% Se_{p_y} 29% subst	1% O_s 99% subst	1% S_{p_y} 99% subst	7% Se_s 39% Se_{p_y} 54% subst
6b	15% O_p 85% subst	40% S_p 20% S_d 40% subst	46% Se_p 12% Se_d 42% subst	70% S_p 9% S_d 21% subst	73% Se_p 6% Se_d 21% subst	4% O_p 96% subst	45% S_p 10% S_d 44% subst	52% Se_p 10% Se_d 38% subst

[a] Subst = substituent on the chalcogenoether.

Table IV. Donor and Acceptor Strengths of Group 15 and 16 Ligands in $(OC)_5Cr-L$ Complexes under Synergic and Nonsynergic Conditions ($L = ER_3$, E = N, P, As, R = H, F; $L = ER_2$, E = S, Se, R = H, F, Me and E = O, R = H, Me)

			nonsynergetic							
			σ-donation		π-acceptance			synergetic		
ligand	ΔE_{prep}, kJ mol^{-1}	$\Delta E^\circ + \Delta E_{res}$, kJ mol^{-1}	electrons	ΔE_σ, kJ mol^{-1}	electrons	ΔE_π, kJ mol^{-1}	ΔE_{syn}, kJ mol^{-1}	σ-donation, electrons	π-acceptance, electrons	ΔH_{LA}, kJ mol^{-1}
CO	15.2	3.9	0.19	057.4	0.17	−66.9	−73.3	0.36	0.31	−178.5
NH_3	0.0	−58.7	0.15	−57.6	–	−5.4	−7.3	0.18	–	−129.0
PH_3	7.4	13.1	0.29	−97.4	0.11	−29.5	−37.9	0.38	0.24	−144.3
AsH_3	10.1	−12.6	0.26	−85.6	0.05	−14.2	−10.1	0.31	0.10	−112.4
NF_3	11.5	69.3	0.11	−43.4	0.11	−80.6	−18.5	0.21	0.18	−61.7
PF_3	14.0	32.9	0.26	−89.3	0.16	−82.6	−38.1	0.44	0.30	−163.1
AsF_3	12.3	60.5	0.21	−71.0	0.12	−54.1	−27.5	0.35	0.23	−79.8
OH_2	0.0	−35.0	0.10	−35.8	–	−2.1	−5.2	0.11	–	−78.1
SH_2	2.5	4.3	0.20	−67.5	0.05	−16.7	−19.2	0.25	0.12	−96.6
SeH_2	2.4	17.3	0.22	−73.4	0.05	−14.7	−25.8	0.30	0.11	−94.2
SF_2	10.9	54.9	0.21	−87.1	0.18	−92.2	055.3	0.39	0.39	−168.8
SeF_2	12.2	65.5	0.23	−97.6	0.16	−76.8	−57.8	0.44	0.39	−154.5
OMe_2	1.7	−37.0	0.09	−35.2	–	1.1	−2.1	0.09	–	−73.7
SMe_2	5.7	−26.5	0.21	−82.8	0.06	−11.0	−14.9	0.26	0.12	−129.5
$SeMe_2$	2.7	−3.9	0.24	−94.9	0.06	−12.3	−19.9	0.31	0.15	−128.3

ability, which is probably caused by the unsuitability of the σ^*-orbitals to accept electron density.

Allowing σ-donation and π-acceptance at the same time enhances the donor and acceptor ability of all ligands studied. The Mulliken population analysis shows that the acceptor strength under synergetic conditions is about doubled, while the donor strength increases only slightly, with the exception of CO, where donor and acceptor ability are doubled. The synergetic effect is particularly large for the fluoro derivatives. For good π-acceptors, like SF_2, SeF_2, and CO, ΔE_{syn} makes a significant contribution to the overall bonding energy ΔH_{LA}. According to our findings, methyl- and hydrogen-substituted chalcogenoethers have to be classified as moderate σ-donors and weak π-acceptors. SF_2 and SeF_2 are good donors and good acceptors, exceeding the widely used CO and PF_3 in donor and acceptor strength. However, steric interactions between the ligand and the metal fragment are responsible for lowering the overall bond energy to a level just below that of CO. The hydrogen-substituted systems SH_2 and SeH_2 have the lowest bond energy ΔH_{LA} and are to be considered weak ligands. SF_2 and SeF_2 are extremely good ligands, and they have to be compared to phosphines in terms of their bonding behavior and bond energy. The somewhat higher bond energies for SMe_2 and $SeMe_2$ are a result of the lower steric repulsion.

The bond length of the metal atom to the trans carbonyl carbon is sensitive to the incoming ligand. For most of the ligands, except SF_2 and SeF_2, a shortening of the $Cr-C_t$ bond length is observed. Changes in the trans carbonyl C–O distance are minor (±0.6 pm) but significant. As expected, for L = NH_3 (II) and OH_2 (V) the $Cr-C_t$ distances are the shortest and hence the C_t-O_t distances are the longest. In the case of good π-acceptors ligands like CO (I) and PF_3 (IX), the $Cr-C_t$ distances are very long and the C_t-O_t distances short. The same is observed for the chalcogen fluoride systems (XI and XII), indicating a strong back-bonding ability of the SF_2 and SeF_2 ligands.

Conclusion

According to our findings, excluding synergetic effects, the following ranking in terms of σ-donor and π-acceptor strength has been obtained:

σ-donor strength:

$$OMe_2 \sim OH_2 < NF_3 < CO \sim NH_3 < SH_2 < AsF_3 \sim SeH_2 < SMe_2 < AsH_3 < SF_2 < PF_3 < SeMe_2 < PH_3 \sim SeF_2$$

π-acceptor strength:

$$OMe_2 \sim OH_2 < NH_3 < SMe_2 < SeMe_2 < AsH_3 < SeH_2 \sim SH_2 < PH_3 < AsF_3 < CO < SeF_2 < NF_3 \sim PF_3 < SF_2$$

Allowing for synergetic interactions enhances the donor and acceptor ability of all systems investigated. Under synergetic conditions the Mulliken populations allow the following ranking in terms of σ-donor and π-acceptor:

σ-donor strength:

$$OMe_2 \sim OH_2 < NH_3 < NF_3 < SH_2 \sim SMe_2 < SeH_2 \sim SeMe_2 \sim AsH_3 < AsF_3 < CO < PH_3 \sim SF_2 < SeF_2 \sim PF_3$$

π-acceptor strength:

$$NH_3 \sim OH_2 \sim OMe_2 < AsH_3 \sim SeH_2 \sim SH_2 \sim SMe_2 < NF_3 < AsF_3 \sim PH_3 < PF_3 \sim CO < SF_2 \sim SeF_2$$

It is the trend that the chromium–chalcogen bond strength increases in the following order: $Cr-EH_2 < Cr-EMe_2 < Cr-EF_2$. The large bond energies found for the fluoro-substituted systems XI and XII suggest that it should be possible to synthesize stable complexes of the unstable molecules SF_2 and SeF_2.

Acknowledgment. This investigation was supported by the Natural Sciences and Engineering Research Council of Canada (NSERC). We thank Professor E. J. Baerends and Professor W. Ravenek for a copy of their vectorized AMOL program system and the University of Calgary for access to their IBM-6000-RISC facilities.

OM920262C